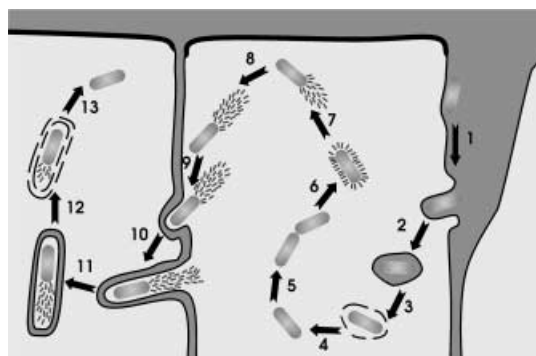


# Structural Aspects of Adhesion to and Invasion of Host Cells by the Human Pathogen *Listeria monocytogenes*

Wolf-Dieter Schubert and Dirk W. Heinz<sup>\*[a]</sup>

## Survey of the listerial infection process

The Gram-positive bacterium *Listeria monocytogenes* is primarily a saprophyte living on decomposing organic matter.<sup>[1]</sup> This mirrors the lifestyle of *Bacillus subtilis*, a soil bacterium to which *Listeria monocytogenes* is genomically closely related.<sup>[2]</sup> In contrast to *B. subtilis*, which as a strict aerobe does not colonize the mammalian gut, *L. monocytogenes* is a facultative intracellular bacterium. It gains access to the gastrointestinal tracts of a wide variety of mammalian hosts, including humans, through consumption of contaminated food. This is a particular problem for the food industry as *L. monocytogenes* is able to survive both at low temperatures and high salt concentrations.<sup>[3]</sup> By recognizing and adhering to epithelial cells lining the intestine, it escapes being expelled from the host intestine by the normal excretory route (Figure 1, step 1). The participation of one



**Figure 1.** The infection cycle of *Listeria monocytogenes*. The bacterium invades various normally non-phagocytic mammalian cell types, including epithelial cells of the intestine. Following uptake, it escapes from the phagosome, moves through the cytosol by actin assembly, and spreads to neighboring cells. See text for details. Adapted from Ref. [59].

listerial surface protein in recognition and adhesion has been particularly well characterized. This molecule alone is necessary and sufficient for the uptake of *L. monocytogenes* into epithelial cell cultures. It was correspondingly termed internalin or InlA.<sup>[4]</sup> Other surface proteins, a class of molecules particularly well represented in *L. monocytogenes*,<sup>[5]</sup> may support this process.<sup>[6]</sup> At the molecular level, InlA recognizes and binds E-cadherin, a mammalian cell-surface protein expressed by intestinal epithelial cells.<sup>[8]</sup> By binding host cellular receptors such as E-cadherin, *L. monocytogenes* physically relays its presence on the outside of

the host cell into an intracellular signal. Existing host cellular signaling pathways and cytoskeletal reorganization mechanisms are thus subverted, inducing the uptake of the bacterium by normally non-phagocytic cells through a process related to phagocytosis (Figure 1, step 2).

Following its phagocytic uptake into the eukaryotic cell, *Listeria monocytogenes* escapes from the resulting phagosome with the help of two secreted phospholipases C, PlcA and PlcB, and listeriolysin, a cytolysin (Figure 1, steps 3 → 4).<sup>[9]</sup> Escape occurs as a prelude to intracellular proliferation (steps 5 → 6) and movement by induced actin polymerization with the help of another listerial surface protein, ActA (steps 7 → 9), and finally cell-to-cell spread (steps 10 → 13).<sup>[10]</sup>

In healthy individuals the listerial infection does not normally spread further than the intestine or possibly the liver and spleen, where the infection is cleared.<sup>[11]</sup> In immunocompromised individuals, however, the infection may spread, infecting various other tissues and causing systemic disease. The uptake into individual cells of these tissues mirrors the initial uptake of *L. monocytogenes* into the intestinal epithelial cells. The involvement of InlA in these secondary tissue infections has not been documented. Instead a second protein, InlB, is involved. Highly similar to InlA (see below), InlB mediates invasion of a wide range of mammalian cells and may be instrumental in enabling *L. monocytogenes* to cross the blood–brain and blood–placental barriers.<sup>[12]</sup>

## The family of internalin proteins

The amino acid sequence of InlA contains two repeat regions, an N-terminal leucine-rich repeat (LRR) domain of fifteen 22-residue repeats (green in Figure 2) and a C-terminal region containing three 70-residue repeats (gray).<sup>[4]</sup> The LRR domain is flanked by two highly conserved domains, an N-terminal cap (yellow) and the so-called “interrepeat” (IR) domain (blue), which physically separates the two repeat regions. At its very N terminus, InlA

[a] Prof. Dr. D. W. Heinz, Dr. W.-D. Schubert  
Department of Structural Biology  
German Research Center for Biotechnology (GBF)  
Mascheroder Weg 1, 38124 Braunschweig (Germany)  
Fax: (+49) 531-6181-763  
E-mail: dih@gbf.de

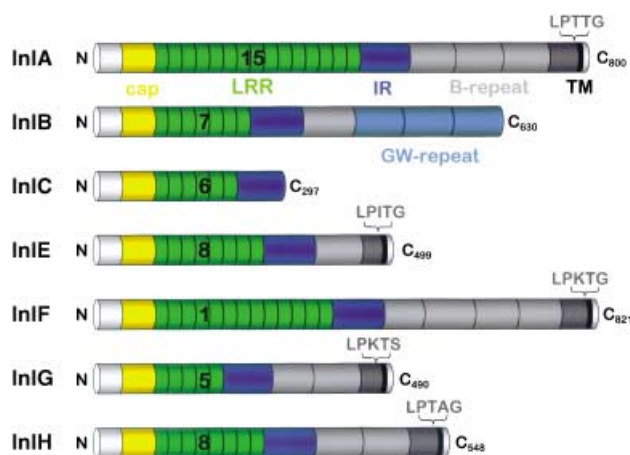


**Figure 2.** The domain structure of the internalin proteins InIA–InIH. All are characterized by a common LRR region (green) and two adjoining domains: an N-terminal cap (yellow) and an “interrepeat” domain (aquamarine). An N-terminal signal peptide (white) and a C-terminal LPxTG-motif, followed by a transmembrane  $\alpha$ -helix and a charged C terminus (all except InIB and InIC) identifies them as surface proteins, covalently bound to the cell wall. InIB reversibly binds to the cell wall lipoteichoic acid through a repeat domain not found in other internalins, while InIC is a secreted protein.

possesses a 35-residue signal peptide (white), which marks the protein for secretion to the bacterial surface. A C-terminal LPxTG motif followed by a hydrophobic, single-pass transmembrane region (black) and a predominantly positively charged tail (white) indicates that InIA is processed by a sortase, SrtA, an enzyme that cleaves the LPxTG motif between T and G and covalently links the protein to the bacterial cell wall, presenting the mature protein on the bacterial cell surface.<sup>[13, 14]</sup>

Immediately downstream of *inIA* is the related gene, *inIB*. It is transcribed both independently of and bicistronically with *inIA*.<sup>[4]</sup> Apart from a similarly strict, 22-residue LRR domain consisting of seven repeats, InIB shares the N-terminal signal peptide with InIA, and also the domains that flank the LRR domain on either side (Figure 2). After a single unit of the C-terminal repeat described for InIA, InIB contains a different, less strongly conserved C-terminal repeat region consisting of three 70- to 85-residue units. InIB also lacks the LPxTG motif and a C-terminal membrane anchor, indicating that the protein is not covalently linked to the cell wall. Instead, the C-terminal repeat motif, also found in other listerial surface proteins such as Ami,<sup>[5]</sup> loosely attaches the protein to lipoteichoic acid in the bacterial cell wall.<sup>[6]</sup>

Yet a third related protein, sharing the signal peptide, the LRR domain consisting of six repeats, and both flanking domains, but lacking all C-terminal extensions, was identified and termed internalin-related protein (IrpA) or InIC.<sup>[15]</sup> Without a cell wall anchoring site, InIC is secreted into the surrounding medium. The genome of *Listeria monocytogenes* encodes for additional related proteins, discovered in due course: InIE (eight repeats), InIF (fourteen), InIG (four), InIH (eight), and InIC2 (seven, a recombination product of InIE and InIH in some strains). All of these proteins share the essential features of InIA, though the number of C-terminal repeat units varies between two and four.<sup>[16, 17]</sup> Other extracellular, listerial proteins also bear LRR

motifs.<sup>[5]</sup> The repeats, however, are significantly less regular and the flanking regions reveal no homology to those described for InIA and InIB. They thus do not cluster with the internalin family of proteins.

## Structures of internalin proteins

The first structural data on internalin proteins were obtained from the crystal structure of the fused cap and LRR domains of InIB,<sup>[18]</sup> followed by the cap/LRR/IR domain structures of InIB and InIH,<sup>[19]</sup> which describe the domains common to all internalins. The array of structures has recently been extended by the structure determination of the cap/LRR/IR domains of InIA,<sup>[19]</sup> a structure of InIB first describing its C-terminal repeats,<sup>[20]</sup> and InIE (this work; Figure 2). In common with other members of the LRR family of proteins,<sup>[21]</sup> the LRR domain of the internalins describes a typical right-handed superhelix. Each repeat consists of a  $\beta$ -strand – loop –  $3_{10}$ -helix – loop motif (Figure 3). Together the LRR units form an elongated, curved, solenoid-like structure, in which the  $\beta$ -strands, oriented perpendicular to the molecular axis, align

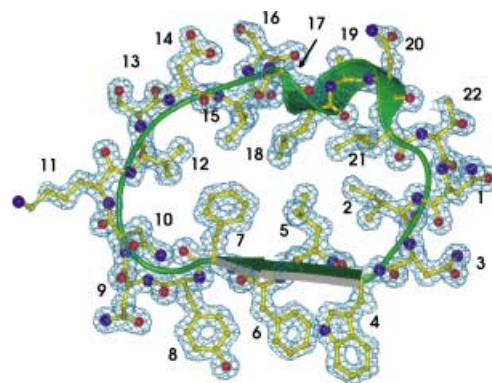


**Figure 3.** A single LRR unit of InIA. Atoms are shown surrounded by their electron density defined at 1.6 Å resolution.<sup>[19]</sup> Individual residues of the 22-residue repeat are numbered. Note the tight packing of carbon atoms (yellow) in the center of the LRR defining the hydrophobic core. A typical ribbon representation is superimposed (green), revealing the location of the  $\beta$ -strand (arrow),  $3_{10}$ -helix, and the intervening loops. The functionally relevant region is located on the outer face of the  $\beta$ -strand. Here an accumulation of aromatic residues aids recognition and adhesion to the hydrophobic N terminus of E-cadherin. All molecular graphics were produced by use of the procedures given in Refs. [60–62], and POV-Ray.

along the concave face to form an extended parallel  $\beta$ -sheet (Figure 4). The  $3_{10}$ -helices are located on the opposite face, creating the outer, convex surface of the molecule. Unlike the first LRR protein described,<sup>[22]</sup> the internalin LRR domain does not curve only around a central point. Instead, each repeat is rotated with respect to its predecessor, introducing an additional twist around the central superhelix axis into the ensemble. Though visible in the shorter members of the internalin family, this effect is more apparent in the longer LRR domains such as in InIH,<sup>[23]</sup> InIE (this work), and especially InIA.<sup>[19]</sup> Structurally, YopM, a virulence factor of *Yersinia pestis*, also falls into this class of LRR proteins.<sup>[24]</sup> The numerous deviations from the 22-residue repeat rule of the LRR of YopM is compensated for by the replacement

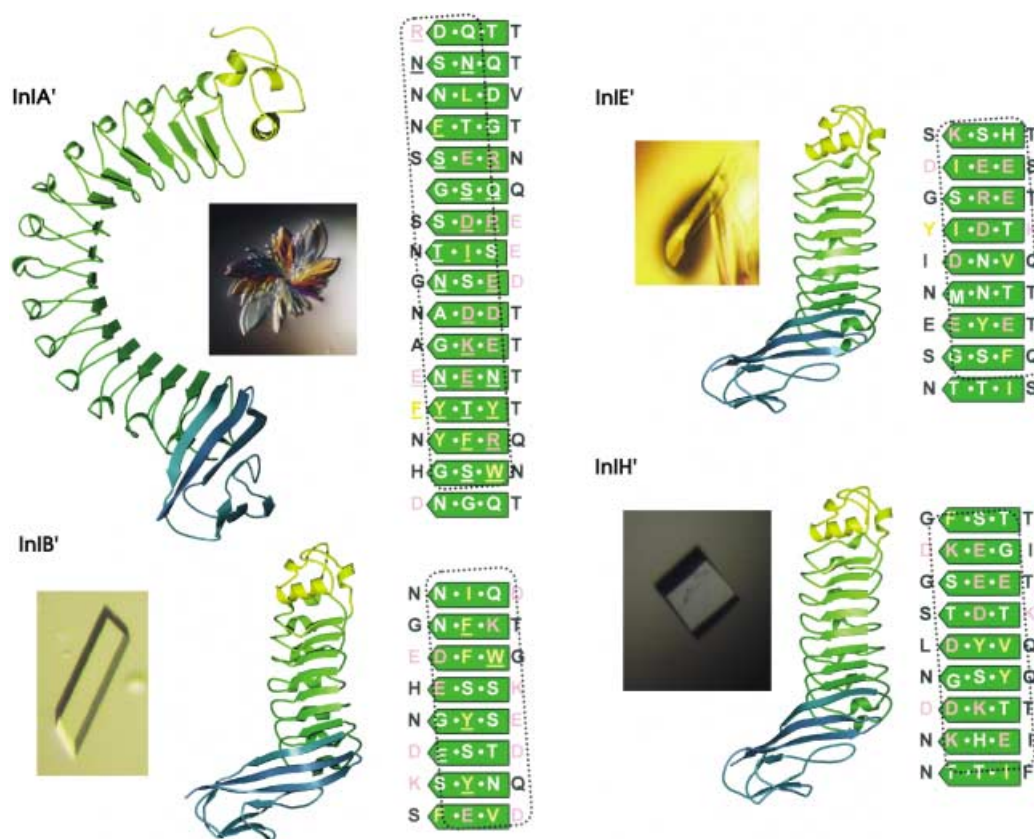


**Figure 4.** The internalin domains of InIA, InIB, InIE, and InIH (denoted InIA', InIB', InIE' and InIH'). Each is represented by a molecular crystal, a "ribbons"-type rendering of the corresponding X-ray structures, and a schematic representation of the (potential) protein–protein interaction surface defined by the parallel  $\beta$ -strand region of the LRR domain. Color coding follows that in Figure 2. In the interaction surface,  $\beta$ -strands are depicted as green arrows pointing left, matching the structural depictions. Lettering is similarly from right to left. Note the unique clustering of hydrophobic (yellow) and charged (pink) residues in each of the four proteins. A dotted rectangle, rotated away from the vertical axis, indicates the residues actually involved in interactions in InIA, caused by the twisting of the LRR. Clustering of functionally relevant residues in this region in other internalins indicates a structurally similar interaction surface.

of the  $3_{10}$ -helix by a non-helical backbone conformation, resulting in both a curvature and a twist very similar to those of the internalin proteins.

At the amino acid level, the LRR-flanking domains are highly conserved in all the internalin proteins. The three-dimensional structures of these domains are correspondingly also very similar (yellow and dark turquoise in Figure 4). Their primary function is clearly to shield the hydrophobic core of the LRR from the aqueous environment, as the spiral nature of the LRR cannot cap itself. By covering this hydrophobic face, the flanking domains significantly enhance the stability of the LRR domain. The cap domain was found structurally to resemble a truncated EF-hand domain first observed in calmodulin, while the IR domain bears some similarity to immunoglobulin (Ig) domains.<sup>[23]</sup> The resemblance to known domains is presumably coincidental, rather than the result of a common evolutionary origin, merely reflecting the functional versatility of such domains. The cap domain advantageously combines a small size with optimal compactness, while the IR- or Ig-related domain—in addition to its capping function—acts as a spacer between the LRR domain and the C-terminal domains. Similar capping domains have been observed in other LRR proteins. In YopM, for example, a similarly

$\alpha$ -helical domain acts as a cap domain,<sup>[24]</sup> though the arrangement of  $\alpha$ -helices bears no resemblance to that in the internalin cap.

Despite its spring-like appearance (Figure 4), the LRR domain appears structurally particularly rigid. This is supported by the fact that identical repeats in different crystalline environments—InIA and InIB have each been crystallized in three unrelated packing arrangements—are surprisingly invariant. This rigidity is achieved both through the highly repetitive and structured hydrophobic core and through the involvement of a conserved asparagine in each repeat, creating an asparagine ladder extending throughout the core of the LRR domain (position 10 in Figure 3). Functionally, this rigidity has the advantage of presenting a constant interaction surface to its binding partner, irrespective of the physical nature of the surrounding medium.

Other than its having fifteen rather than seven LRR units, the structure of InIA', the functional cap/LRR/IR domain of InIA (see below), is in principle not very different from that of InIB' (Figure 4). The larger number of repeats creates a significantly stronger curvature (roughly  $170^\circ$ ) and accentuates the inherent twist of InIA'. However, a single repeat, LRR6 of InIA, deviates from the strict consensus of 22-residues observed for all other



internalins: here residue 8, located at the C-terminal tip of the  $\beta$ -strand, is deleted. This deletion is different from the repeats shorter than 22 residues observed in YopM, as such deletions always occur away from the  $\beta$ -strand. Whereas the central  $\beta$ -sheet of YopM is indistinguishable from the standard internalin  $\beta$ -sheet geometry, the deletion in InIA upsets the regular  $\beta$ -sheet here, introducing a notable kink into the extended molecule. The resulting small hydrophobic depression in the surface of the LRR domain is vital to its function (see below), as it accommodates a proline residue of the E-cadherin host receptor and upsets the rigidity of the LRR sufficiently to allow some structural adjustment during receptor binding.<sup>[19]</sup>

### Listerial infection in the intestine: structure of the InIA – E-cadherin complex

Possibly the first directed step in the listerial infection process is the specific recognition of intestinal epithelial cells by *Listeria monocytogenes*, leading to adhesion and invasion. On the molecular level this is achieved by the listerial surface protein InIA recognizing mammalian E-cadherin.<sup>[8]</sup> E-cadherin is a member of the large class of single-pass transmembrane receptors.<sup>[25]</sup> It is composed of five extracellular domains, a transmembrane  $\alpha$ -helix, and an extended cytosolic C-terminal stretch.<sup>[26]</sup> Structurally, the extracellular domains each adopt an Ig-related fold,<sup>[27–29]</sup> while the C-terminal domain is presumably structured only when bound to its recognition partner  $\beta$ -catenin<sup>[26, 30]</sup> or the related plakoglobin ( $\gamma$ -catenin).<sup>[31]</sup> Physiologically, the role of E-cadherin is to ensure cell–cell adhesion through homotopic recognition of E-cadherin molecules on neighboring cells.<sup>[32]</sup> The cumulative effect of numerous such complexes fuses neighboring cells over large regions of their surface area. Through successive interactions of  $\beta$ -catenin with  $\alpha$ -catenin,  $\alpha$ -catenin with  $\alpha$ -actinin, vinculin and other adaptor proteins, E-cadherin provides a point of actin cytoskeleton attachment. Overall, the fused cell surfaces together with the linked complex create the so-called adherens junction.<sup>[32]</sup>

In vivo and in vitro studies had previously indicated that the LRR domain of InIA is necessary and sufficient for complex formation, whereas in the case of E-cadherin only the N-terminal domain is required.<sup>[8]</sup> The smallest stable protein constructs were thus engineered, to investigate their interaction further. In the case of InIA, this involved the fused N-terminal domains, the cap, LRR, and Ig-like domains. This construct we term InIA'. For human E-cadherin the N-terminal domain (residues 1–100, termed hEC1) was found to be stable and soluble on its own.<sup>[19]</sup>

Analytical ultracentrifugation revealed a dissociation constant of  $50 \pm 30 \mu\text{M}$  for the two molecules in the absence of  $\text{Ca}^{2+}$  and  $8 \pm 4 \mu\text{M}$  in the presence of  $10 \text{ mM Ca}^{2+}$ .<sup>[19]</sup> This indicates a relatively weak interaction. The crystal structure confirms the interaction, revealing that hEC1 occupies the central void of InIA' (Figure 5). The latter wraps around the smaller hEC1, creating an extended, curved contact interface involving numerous individual residues of hEC1 located along its circumference. Most intermolecular interactions exclusively involve side-chain atoms of InIA', while both backbone and side-chain atoms are involved in hEC1. Although only  $\beta$ -strand regions from both proteins are

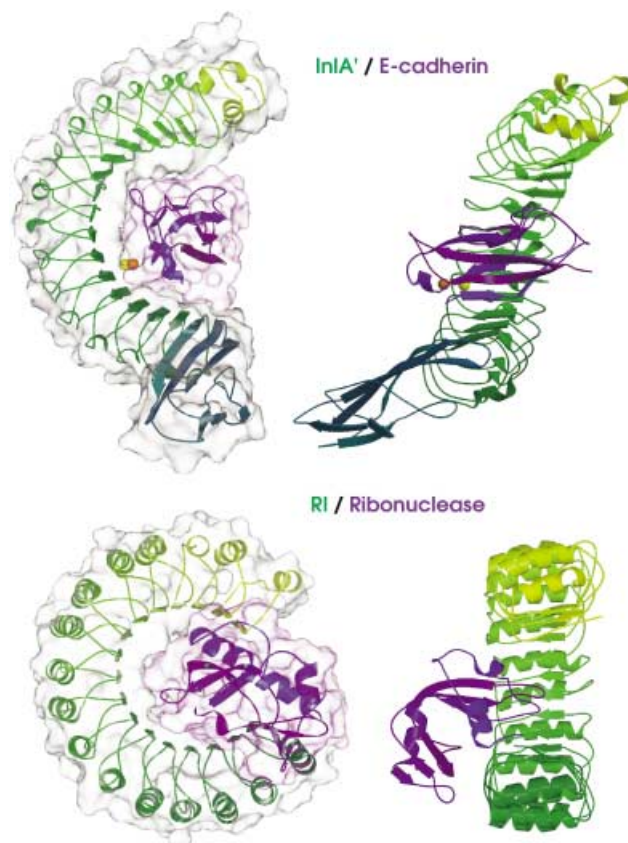


**Figure 5.** Top: The complex of the functional domains of InIA (denoted InIA') (yellow, green, aquamarine) from *Listeria monocytogenes* and human E-cadherin (purple). Left: The protein backbones are depicted schematically, while the translucent surfaces give an impression of the extended surface of interaction between the two molecules. Note the bridging position of  $\text{Ca}^{2+}$  (orange sphere) and  $\text{Cl}^-$  (yellow) between the two. Right: The protein complex is rotated by  $180^\circ$  around the vertical axis. The N-terminal domain hEC1 of E-cadherin recognized by InIA is located at the center of the surrounding embrace. Bottom, Left: The complex between the porcine ribonuclease inhibitor (RI, colors similar to InIA') and ribonuclease (purple).<sup>[36]</sup> Right: Rotated by  $180^\circ$ . The ribonuclease is located adjacent to the central LRR plane. Despite the obvious analogy between the two LRR proteins, each is optimized to achieve a unique interaction, distinct from the other.

involved in the interaction, pairing of  $\beta$ -strands from the different proteins is thus not possible. The only region of InIA where backbone atoms hydrogen bond to hEC1 involves a hydrophobic pocket in LRR5 to LRR7. This pocket, near the C-terminal end of the  $\beta$ -strands, results from a single amino acid deletion in LRR6, reducing the 22-residue consensus length of this repeat to 21. The regular LRR arrangement is thereby disturbed locally, introducing a noticeable kink into the LRR domain (see above). The hydrophobic pocket, though not particularly deep, is sufficient to accommodate Pro16 of hEC1. Pro16 is located at the tip of an extended loop and adopts a *cis* conformation, causing it to protrude from the general globular shape of hEC1. This structural feature of hEC1 is probed by InIA, ensuring specific recognition between the two proteins. Pro16 had in fact previously been identified as crucial to the recognition of E-cadherin by InIA. Its replacement by Glu16 in murine E-cadherin renders mice largely insensitive to oral

challenge by *Listeria monocytogenes*.<sup>[33]</sup> Expression of human E-cadherin by transgenic mice correspondingly abolishes this natural immunity, creating a suitable mouse model for human listeriosis.<sup>[34]</sup>

A second major part of InIA' involved in recognizing hEC1 includes a patch of hydrophobic, mainly aromatic, residues in LRRs 13, 14, and 15. These residues are in contact mainly with the N-terminal  $\beta$ -strand of hEC1, which is much more closely associated with the remaining domain than in any other crystal structure involving the N-terminal domain of E-cadherin.<sup>[26–29]</sup> Although the interaction does not appear particularly specific, replacement of any one of the hydrophobic InIA residues by serine reduces binding affinity to hEC1 to such an extent that it is no longer observable by analytical ultracentrifugation.<sup>[19]</sup>

Overall, the arrangement of InIA'/hEC1 is clearly analogous to that of the complex between the porcine ribonuclease inhibitor (RI) and ribonuclease,<sup>[36]</sup> where a smaller protein domain is recognized by a surrounding LRR molecule (Figure 5, bottom). However, the dissociation constant of the latter complex differs by many orders of magnitude, indicating a very much tighter interaction. The RI/ribonuclease complex indicates that a higher binding affinity is in principle possible in such a system. The fact that the binding affinity is so low could indicate that InIA has multiple targets that, apart from E-cadherin, have not been identified. This would mirror the recognition of both ribonuclease and angiogenin by the ribonuclease inhibitor<sup>[37]</sup> and the multiple binding partners of InIB (see below)—though only one of these is known to involve the LRR domain. Nevertheless, the binding affinity for each partner needs to remain physiologically relevant. As InIA is able to induce bacterial uptake, weak binding is clearly not a result of “poor design” but rather achieves a critical balance between complex formation and dissociation. Instead, multiple copies of both InIA and E-cadherin would allow the formation of numerous complexes, which would add cooperatively to the overall strength of *Listeria* attachment to the host cell.

Correspondingly, millimolar concentrations of  $\text{Ca}^{2+}$  were found to impact significantly on the binding affinity between InIA' and hEC1, improving the affinity constant by one order of magnitude (see above). In the crystal structure of InIA' and hEC1, a discrete  $\text{Ca}^{2+}$ -binding site was identified in the interface of both proteins. It bridges two acidic residues, Glu326 of InIA' and Asp29 of hEC1, the latter residue through two water molecules (orange sphere in Figure 5, top).<sup>[19]</sup> As the intracellular  $\text{Ca}^{2+}$  concentration (nanomolar range) is known to be several orders of magnitude lower than that of the extracellular environment and the intestinal lumen (millimolar range), extracellular binding between InIA and E-cadherin is enhanced in relation to an intracellular environment. Macroscopically, this allows complex formation and bacterial adhesion on the exterior of the cell, while falling  $\text{Ca}^{2+}$  concentration in the punctured phagosome following phagocytosis (Figure 1, step 3) leads to complex dissociation and bacterial release from the surrounding membrane. In addition to the direct bridging role,  $\text{Ca}^{2+}$  was also found to be required for the loop of hEC1 containing Pro16 to adopt a rigid conformation.<sup>[27]</sup> Conserved  $\text{Ca}^{2+}$  binding sites between extracellular domains furthermore ensure an overall extended

conformation of E-cadherin.<sup>[38, 39]</sup> Interaction between InIA and E-cadherin is thus multiply dependent on  $\text{Ca}^{2+}$ , ensuring that a decrease in its concentration will significantly destabilize the interaction between the two.

How does binding of InIA to E-cadherin induce “zipper”-like phagocytosis? The crystal structure of InIA' and hEC1 indicates that no structural rearrangement of hEC1 that could have been transmitted through the membrane to the cytoplasmic domain of E-cadherin is immediately obvious.<sup>[19]</sup> InIA-induced uptake appears to involve the unconventional myosin VIIA present in the cytosol of the host cell.<sup>[40, 41]</sup> However, this does not imply that its involvement is specifically induced by InIA. Instead, it may be hypothesized that bacterial adhesion could induce clustering of E-cadherin through a high local concentration of InIA, simulating formation of a nascent adherens junction. This would induce intracellular actin polymerization and cytoskeletal tension required for normal cell rigidity through the involvement of myosin VIIA. It may thus be envisaged that spatially limited clustering of E-cadherin could pull the bacterium into the eukaryotic cell while the distribution of InIA over the bacterial cell surface would extend the area of interaction finally to cover the entire bacterium, completing the process of engulfment.<sup>[19, 40]</sup> In this way, no InIA-specific signaling is required for bacterial uptake. A similar bacterial subversion tactic may underlie uptake of other human pathogens such as *Yersinia* and *Staphylococcus*. Each presents on its cell surface a dedicated adhesin that either competes with fibronectin for the extracellular region of eucaryotic integrins (invasin in *Yersinia*)<sup>[42]</sup> or alternatively targets integrins indirectly by binding fibronectin through fibronectin-binding proteins (*Staphylococcus*)<sup>[43]</sup> and relying on the physiological recognition between fibronectin and integrin. In either case, clustering of integrin would simulate nascent extracellular matrix-recognition, inducing cytoskeletal tension normally required to allow cell attachment or locomotion. Analogously to the InIA/E-cadherin system, the spatially limited extent of the interaction would subvert the pre-programmed tensile force to initiate bacterial phagocytosis into normally non-phagocytic cells.

### InIB-dependent uptake of *Listeria monocytogenes*

The function of InIB mirrors that of InIA in similarly inducing uptake of entire bacteria by host cells.<sup>[44–46]</sup> Apart from epithelial cells, the spectrum of host cell lines infected by InIB additionally includes hepatocytes, fibroblasts, and endothelial cells.<sup>[44, 47–49]</sup> While the physiological function of InIA appears to be initial bacterial uptake in the intestine, InIB, by inducing uptake into other tissues, aids bacterial dissemination once infection has occurred.<sup>[50]</sup> InIB-induced internalization was observed to resemble the phagocytic-like “zipper” mechanism brought about by intracellular rearrangement of the cytoskeleton.<sup>[46]</sup> Soluble InIB furthermore induces membrane ruffling and cell scattering, phenomena reminiscent of growth factors.<sup>[51]</sup> This led to the identification of the probable main receptor of InIB, the protooncogene c-Met or hepatocyte growth factor (HGF) receptor tyrosine kinase.<sup>[51]</sup>

Met is a disulfide-linked  $\alpha/\beta$  heterodimer, synthesized as a single-chain precursor but proteolytically cleaved during maturation to yield an extracellular, 50 kDa  $\alpha$ -chain and a single pass, 145 kDa transmembrane  $\beta$ -chain bearing a cytoplasmic tyrosine kinase domain.<sup>[52]</sup> As in other receptor tyrosine kinases, ligand binding to the extracellular domain of Met is presumably relayed through the cell membrane, possibly by receptor dimerization, resulting in the autophosphorylation of tyrosine residues in the C-terminal domain of the receptor. Tyrosine phosphorylation allows intracellular proteins to bind to the receptor, causing further activation or inhibition of downstream signaling cascades. The structure of Met, including any binding sites and modes of activation or dimerization, is currently largely unknown. Nevertheless, despite the resemblance of InlB-induced responses to those of HGF,<sup>[51, 53]</sup> these ligands do not compete for the same binding site.<sup>[51]</sup> Binding of InlB is dependent only on its LRR domain, not on the C-terminal domains.<sup>[53]</sup> In fact, the dissociation constant of InlB' (the N-terminal half of InlB, residues 36 to 321) and the extracellular domain of Met was found to be in the range of 20–30 nM,<sup>[54]</sup> while that of HGF and Met is 20–70 pM,<sup>[55, 56]</sup> indicating that InlB' and HGF both bind tightly to Met. The X-ray structure of InlB' reveals the prominent positioning of a group of aromatic (hydrophobic) amino acid residues—Phe104, Trp124, Phe126, and Tyr170 or Tyr214—on the concave surface of the LRR domain (Figure 6).<sup>[18, 23]</sup> Replacement of these either individually or cumulatively by serine severely reduces the binding affinity of the resulting InlB'-variants for Met and abrogates uptake of InlB'-covered latex beads—except, that is, for Phe126, which despite its central

location does not appear to be directly involved in binding Met.<sup>[54]</sup> The hydrophobic residues are thus directly involved in binding to the extracellular domain of Met, leading to InlB-induced uptake—at least of coated beads.<sup>[54]</sup> In vivo assays employing single-exchange, of full-length InlB variants in *Listeria monocytogenes* indicate that here the effect of individual residues is not as strong. Cumulative replacement of three to five aromatic residues is required to down-regulate invasion of HeLa cells significantly.<sup>[54]</sup>

In addition to binding of Met, InlB binds at least one other distinct host cell receptor: gC1q-R.<sup>[57]</sup> This recognition, however, does not involve the LRR domain of InlB, but rather the C-terminal repeat region.<sup>[58]</sup> This domain thus has multiple functions, as it is involved in reversible attachment of InlB to the lipoteichoic acid of the cell wall of *Listeria monocytogenes*<sup>[6]</sup> and has been shown to bind to the glycosaminoglycan heparin on the cell membrane of eukaryotic cells.<sup>[58]</sup>

Structurally, the C-terminal domain is related to SH3 domains (Figure 6, inset).<sup>[20]</sup> This may document an ancient evolutionary relationship, though, as with the domains flanking the LRR of the internalin proteins, the function is unrelated to that of structurally homologous domains. Instead, the domain is presumably optimized to bind its disparate ligands, though the structural aspects of this recognition currently remain unclear.

Functionally, the reversible binding of InlB to the bacterial cell wall helps to maintain a high concentration of this protein in the immediate vicinity of the bacterial surface, ensuring that membrane ruffling will only occur in close proximity to the bacterium. By dissociating from the cell wall and associating with heparin of the target cell, simulating the behavior of HGF, a closely localized concentration of InlB is maintained, leading to a spatially limited, optimally coordinated induction of signaling through Met. Furthermore, the tight binding of InlB to Met<sup>[54]</sup> ensures that the outside-in signal through Met is maintained at near maximum levels, as long as it is required.

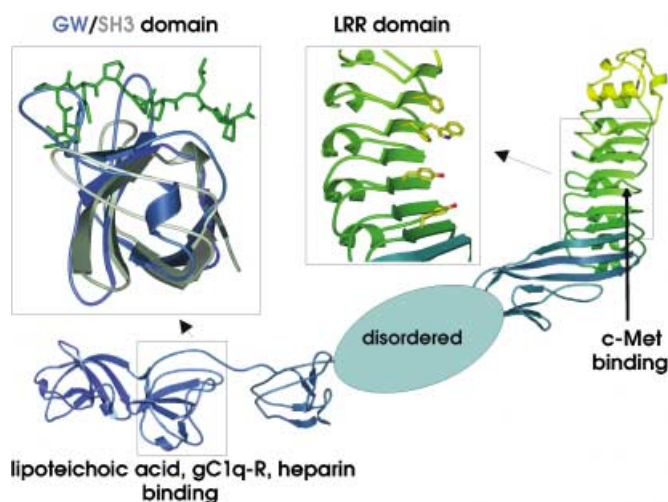


**Figure 6.** The crystal structure of the complete InlB molecule.<sup>[20]</sup> The internalin domain (colors as in Figure 4) and the C-terminal, cell wall-anchoring (GW) repeat domain (blue) of InlB combine to create an extended molecule. The intermediate domain, homologous to the C-terminal repeat unit of most other internalins, was disordered in the crystal structure and could not be modeled. Its approximate size is indicated by a blue-gray ellipsoid. Left inset: An enlargement of the C-terminal repeat domain of InlB (blue) in comparison to the SH3 domain of the Abl tyrosine kinase<sup>[63]</sup> (gray, green). Note that despite the overall structural similarity, the polyproline-binding pocket of typical SH3 domains is blocked by extended loops in the InlB GW domain. Right inset: The aromatic residues on the concave side of the LRR domain of InlB directly participate in binding the c-Met receptor tyrosine kinase.<sup>[54]</sup>

### Internalins as tools to study host cell function

InlA and InlB are both potent pathogenicity factors that achieve efficient uptake of whole bacteria into normally nonphagocytic eukaryotic cells. Each, at least in vitro, functions independently of any other bacterial proteins, allowing listerial uptake into a large array of eukaryotic cells. Interestingly, they employ two independent routes of subterfuge to achieve similar final outcomes: InlB binds to Met, inducing classical receptor tyrosine kinase signaling pathways, whilst InlA more succinctly may subvert a process aimed at cell and tissue maintenance to induce its own form of phagocytosis. Though each process functions independently of the other, they may be employed in parallel in vivo, potentiating their respective efficiencies.<sup>[6]</sup> Mechanisms underlying both InlA- and InlB-mediated phagocytosis are currently only incompletely understood. Both are therefore potentially invaluable tools for cell biology in further investigation of these complex eukaryotic processes.

**Keywords:** cell adhesion • E-cadherin • internalins • invasion • *Listeria monocytogenes* • protein structures

- [1] J. A. Vazquez-Boland, M. Kuhn, P. Berche, T. Chakraborty, G. Dominguez-Bernal, W. Goebel, B. Gonzalez-Zorn, J. Wehland, J. Kreft, *Clin. Microbiol. Rev.* **2001**, *14*, 584–640.
- [2] P. Glaser, L. Frangeul, C. Buchrieser, C. Rusniok, A. Amend, F. Baquero, P. Berche, H. Bloecker, P. Brandt, T. Chakraborty, A. Charbit, F. Chetouani, E. Couvé, A. de Daruvar, P. Dehoux, E. Domann, G. Domínguez-Bernal, E. Duchaud, L. Durant, O. Dussurget, K.-D. Entian, H. Fsihi, F. Garcia-Del Portillo, P. Garrido, L. Gautier, W. Goebel, N. Gómez-López, T. Hain, J. Hauf, D. Jackson, L.-M. Jones, U. Kaerst, J. Kreft, M. Kuhn, F. Kunst, G. Kurapkat, E. Madueño, A. Maitournam, J. Mata Vicente, E. Ng, H. Nedjari, G. Nordsiek, S. Novella, B. de Pablos, J.-C. Pérez-Díaz, R. Purcell, B. Rimmel, M. Rose, T. Schlueter, N. Simoes, A. Tierrez, J.-A. Vázquez-Boland, H. Voss, J. Wehland, P. Cossart, *Science* **2001**, *294*, 849–852.
- [3] J. M. Farber, P. I. Peterkin, *Microbiol. Rev.* **1991**, *55*, 476–511.
- [4] J. L. Gaillard, P. Berche, C. Frehel, E. Gouin, P. Cossart, *Cell* **1991**, *65*, 1127–1141.
- [5] D. Cabanes, P. Dehoux, O. Dussurget, L. Frangeul, P. Cossart, *Trends Microbiol.* **2002**, *10*, 238–245.
- [6] R. Jonquieres, H. Bienne, F. Fiedler, P. Gounon, P. Cossart, *Mol. Microbiol.* **1999**, *34*, 902–914.
- [7] B. Bergmann, D. Raffelsbauer, M. Kuhn, M. Goetz, S. Hom, W. Goebel, *Mol. Microbiol.* **2002**, *43*, 557–570.
- [8] J. Mengaud, H. Ohayon, P. Gounon, R. M. Mege, P. Cossart, *Cell* **1996**, *84*, 923–932.
- [9] S. Dramsi, P. Cossart, *J. Cell Biol.* **2002**, *156*, 943–946.
- [10] P. Cossart, H. Bienne, *Curr. Opin. Immunol.* **2001**, *13*, 96–103.
- [11] L. P. Cousins, E. J. Wing, *Immunol. Rev.* **2000**, *174*, 150–159.
- [12] H. Bienne, P. Cossart, *J. Cell Sci.* **2002**, *115*, 3357–3367.
- [13] C. Garandeau, H. Reglier-Poupet, I. Dubail, J. L. Beretti, P. Berche, A. Charbit, *Infect. Immun.* **2002**, *70*, 1382–1390.
- [14] H. Bienne, S. K. Mazmanian, M. Trost, M. G. Pucciarelli, G. Liu, P. Dehoux, L. Jänsch, F. Garcia-del Portillo, O. Schneewind, P. Cossart, *Mol. Microbiol.* **2002**, *43*, 869–881.
- [15] E. Domann, S. Zechel, A. Lingnau, T. Hain, A. Darji, T. Nichterlein, J. Wehland, T. Chakraborty, *Infect. Immun.* **1997**, *65*, 101–109.
- [16] S. Dramsi, P. Dehoux, M. Lebrun, P. L. Goossens, P. Cossart, *Infect. Immun.* **1997**, *65*, 1615–1625.
- [17] D. Raffelsbauer, A. Bubert, F. Engelbrecht, J. Scheinplflug, A. Simm, J. Hess, S. H. E. Kaufmann, W. Goebel, *Mol. Gen. Genet.* **1998**, *260*, 144–158.
- [18] M. Marino, L. Braun, P. Cossart, P. Ghosh, *Mol. Cell* **1999**, *4*, 1063–1072.
- [19] W.-D. Schubert, C. Urbanke, T. Ziehm, V. Beier, M. P. Machner, E. Domann, J. Wehland, T. Chakraborty, D. W. Heinz, *Cell* **2002**, *111*, 825–836.
- [20] M. Marino, M. Banerjee, R. Jonquieres, P. Cossart, P. Ghosh, *EMBO J.* **2002**, *21*, 5623–5634.
- [21] B. Kobe, A. V. Kajaia, *Curr. Opin. Struct. Biol.* **2001**, *11*, 725–732.
- [22] B. Kobe, J. Deisenhofer, *Nature* **1993**, *366*, 751–756.
- [23] W.-D. Schubert, G. Göbel, M. Diepholz, A. Darji, D. Kloer, T. Hain, T. Chakraborty, J. Wehland, E. Domann, D. W. Heinz, *J. Mol. Biol.* **2001**, *312*, 783–794.
- [24] A. G. Evdokimov, D. E. Anderson, K. M. Routzahn, D. S. Waugh, *J. Mol. Biol.* **2001**, *312*, 807–821.
- [25] B. D. Angst, C. Marozzi, A. I. Magee, *J. Cell. Sci.* **2001**, *114*, 629–641.
- [26] A. H. Huber, W. I. Weis, *Cell* **2001**, *105*, 391–402.
- [27] L. Shapiro, A. M. Fannon, P. D. Kwong, A. Thompson, M. S. Lehmann, G. Grubel, J. F. Legrand, J. Als-Nielsen, D. R. Colman, W. A. Hendrickson, *Nature* **1995**, *374*, 327–337.
- [28] M. Overduin, T. S. Harvey, S. Bagby, K. I. Tong, P. Yau, M. Takeichi, M. Ikura, *Science* **1995**, *267*, 386–389.
- [29] T. J. Boggon, J. Murray, S. Chappuis-Flament, E. Wong, B. M. Gumbiner, L. Shapiro, *Science* **2002**, *296*, 1308–1313.
- [30] A. H. Huber, D. B. Stewart, D. V. Laurents, W. J. Nelson, W. I. Weis, *J. Biol. Chem.* **2001**, *276*, 12301–12309.
- [31] A. S. Yap, W. M. Brieher, B. M. Gumbiner, *Annu. Rev. Cell Dev. Biol.* **1997**, *13*, 119–146.
- [32] A. Nagafuchi, *Curr. Opin. Cell Biol.* **2001**, *13*, 600–603.
- [33] M. Lecuit, S. Dramsi, C. Gottardi, M. Fedor-Chaiken, B. Gumbiner, P. Cossart, *EMBO J.* **1999**, *18*, 3956–3963.
- [34] M. Lecuit, S. Vandormael-Pournin, J. Lefort, M. Huerre, P. Gounon, C. Dupuy, C. Babinet, P. Cossart, *Science* **2001**, *292*, 1722–1725.
- [35] O. Pertz, D. Bozic, A. W. Koch, C. Fauser, A. Brancaccio, J. Engel, *EMBO J.* **1999**, *18*, 1738–1747.
- [36] B. Kobe, J. Deisenhofer, *Nature* **1995**, *374*, 183–186.
- [37] A. C. Papageorgiou, R. Shapiro, K. R. Acharya, *EMBO J.* **1997**, *16*, 5162–5177.
- [38] S. Pokutta, K. Herrenknecht, R. Kemler, J. Engel, *Eur. J. Biochem.* **1994**, *223*, 1019–1026.
- [39] B. Nagar, M. Overduin, M. Ikura, J. M. Rini, *Nature* **1996**, *380*, 360–364.
- [40] P. Cossart, J. Pizarro-Cerda, M. Lecuit, *Trends Cell Biol.* **2003**, *13*, 23–31.
- [41] C. R. Roy, F. Gisou van der Goot, *Nature Cell Biol.* **2003**, *5*, 16–19.
- [42] Z. A. Hamburger, M. S. Brown, R. R. Isberg, P. J. Borkman, *Science* **1999**, *286*, 291–295.
- [43] U. Schwarz-Linek, J. M. Werner, A. R. Pickford, S. Gurusiddappa, J. H. Kim, E. S. Pilka, J. A. Briggs, T. S. Gough, M. Hook, I. D. Campbell, J. R. Potts, *Nature* **2003**, *423*, 177–181.
- [44] S. Dramsi, I. Biswas, E. Maguin, L. Braun, P. Mastroeni, P. Cossart, *Mol. Microbiol.* **1995**, *16*, 251–261.
- [45] L. Braun, S. Dramsi, P. Dehoux, H. Bienne, G. Lindahl, P. Cossart, *Mol. Microbiol.* **1997**, *25*, 285–294.
- [46] L. Braun, H. Ohayon, P. Cossart, *Mol. Microbiol.* **1998**, *27*, 1077–1087.
- [47] K. Ireton, B. Payastre, H. Chap, W. Ogawa, H. Sakaue, M. Kasuga, P. Cossart, *Science* **1996**, *274*, 780–782.
- [48] S. K. Parida, E. Domann, M. Rohde, S. Müller, A. Darji, T. Hain, J. Wehland, T. Chakraborty, *Mol. Biobiol.* **1998**, *28*, 81–93.
- [49] L. Greiffenberg, W. Goebel, K. S. Kim, I. Weiglein, A. Bubert, F. Engelbrecht, M. Stins, M. Kuhn, *Infect. Immun.* **1998**, *66*, 5260–5267.
- [50] J. L. Gaillard, F. Jaubert, P. Berche, *J. Exp. Med.* **1996**, *183*, 359–369.
- [51] Y. Shen, M. Naujokas, M. Park, K. Ireton, *Cell* **2000**, *103*, 501–510.
- [52] S. Giordano, M. F. Di Renzo, R. P. Narsimhan, C. S. Cooper, C. Rosa, P. M. Comoglio, *Oncogene* **1989**, *4*, 1383–1388.
- [53] L. Braun, F. Nato, B. Payastre, J. C. Mazie, P. Cossart, *Mol. Microbiol.* **1999**, *34*, 10–23.
- [54] M. P. Machner, S. Frese, H. H. Niemann, W.-D. Schubert, V. Orian-Rousseau, J. Wehland, D. W. Heinz, *Mol. Microbiol.* **2003**, *48*, 1525–1536.
- [55] M. Komada, K. Miyazawa, T. Ishii, N. Kitamura, *Eur. J. Biochem.* **1992**, *204*, 857–864.
- [56] H. Tajima, O. Higuchi, K. Mizuno, T. Nakamura, *J. Biochem.* **1992**, *111*, 401–406.
- [57] L. Braun, B. Ghebrehewet, P. Cossart, *EMBO J.* **2000**, *19*, 1458–1466.
- [58] R. Jonquieres, J. Pizarro-Cerda, P. Cossart, *Mol. Microbiol.* **2001**, *42*, 955–965.
- [59] L. G. Tilney, D. A. Portnoy, *J. Cell Biol.* **1989**, *109*, 1597–1608.
- [60] P. J. Kraulis, *J. Appl. Crystallogr.* **1991**, *24*, 946–950.
- [61] A. Nicholls, R. Bharadwaj, B. Honig, *Biophys. J.* **1993**, *64*, A166.
- [62] E. A. Merritt, D. J. Bacon, *Methods Enzymol.* **1997**, *277*, 505–524.
- [63] A. Musacchio, M. Saraste, M. Wilmanns, *Nat. Struct. Biol.* **1994**, *1*, 546–551.

Received: April 16, 2003 [M624]